The Crystal Structure of Fragment Double-D from Cross-Linked Lamprey Fibrin Reveals Isopeptide Linkages across an Unexpected D−D Interface[†,‡]

Zhe Yang,[§] Leela Pandi, and Russell F. Doolittle*

Center for Molecular Genetics, University of California at San Diego, La Jolla, California 92093-0634

Received August 17, 2002; Revised Manuscript Received October 29, 2002

ABSTRACT: The crystal structure of fragment double-D from factor XIII-cross-linked lamprey fibrin has been determined at 2.9 Å resolution. The 180 kDa covalent dimer was cocrystallized with the peptide Gly-His-Arg-Pro-amide, which in many fibrinogens, but not that of lamprey, corresponds to the B-knob exposed by thrombin. The structure was determined by molecular replacement, a recently determined structure of lamprey fragment D being used as a search model. GHRPam was found in both the γ- and β-chain holes. Unlike the situation with fragment D, the crystal packing of the cross-linked double-D structure exhibits two different D−D interfaces, each γ-chain facing γ-chains on two other molecules. One of these (interface I) involves the asymmetric interface observed in all other D fragments and related structures. The other (interface II) encompasses a completely different set of residues. The two abutments differ in that interface I results in an "in line" arrangement of abutting molecules and the interface II in a "zigzag" arrangement. So far as can be determined (the electron density could only be traced on one side of the cross-links), it is the γ-chains of the newly observed zigzag units (interface II) that are joined by the reciprocal ϵ-amino-γ-glutamyl cross-links. Auspiciously, the same novel D−D interface was observed in two lower-resolution crystal structures of human double-D preparations that had been crystallized under unusual circumstances. These observations show that double-D structures are linked in a way that is sufficiently flexible to accommodate different D−D interfaces under different circumstances.

A principal goal in studying the three-dimensional structures of fibrinogen and its fragments remains the elucidation of how the units fit together in the fibrin clot. Significant progress toward that goal was realized with the first crystal structure of the 170 kDa entity called "double-D" (also called "D-dimer") isolated by proteolytic digestion of naturally cross-linked fibrin (*1*). The structure revealed an offset, end-to-end abutment between fragment D units that was in good accord with longstanding notions of how fibrin monomers are organized, including considerable support from biochemistry, electron microscopy, and genetics. Much of the history of these developments can be found in two comprehensive symposium volumes (*2*, *3*).

In this regard, it has been predicated for half a century that fibrin polymerization occurs by a kind of half-staggered overlap that initially forms a two-molecule thick, end-to-end polymer called a protofibril (*4*). The initial association is promoted by thrombin unmasking "knobs" in the central domains of fibrinogen that can interact with ever-present "holes" near the extremities of neighboring molecules (reviewed in ref *5*). Thus, pairs of knobs from the fragment E region of one molecule hold together the fragment D ends of other molecules, the boundary between the pinned-together molecules being known as the "D−D interface". Synthetic peptides patterned on knob sequences can inhibit these initial interactions (*6*, *7*).

Although these early associations are completely noncovalent, under physiological conditions the transglutaminase known as factor XIII introduces covalent cross-links between the newly associated units. Thus, reciprocal ϵ-amino-γ-glutamyl cross-links form between the carboxyl-terminal segments of γ-chains (*8*). Unfortunately, none of the several crystal structures of double-D reported so far (*1*, *9*, *10*) has shown the cross-links, the conclusion being that the links, like the unlinked γ-chain segments (*1*, *11*), are flexible and too mobile to resolve.

Recently, we reported the crystal structure of a fragment D from lamprey fibrinogen that had been cocrystallized with the peptide Gly-His-Arg-Pro-amide (*12*). Although the overall structure differed only slightly from previously determined fragment D structures from human fibrinogen, it did have a better resolved γ-chain carboxyl-terminal segment. This led us to crystallize the equivalent cross-linked fragment from lamprey fibrin, our hope being that the elusive cross-linked terminal segments might finally be observed. These hopes have been partly realized. As it happens, however, the packing in the lamprey double-D crystals is quite different than that observed in lamprey fragment D prepared under the same conditions, a second D−D interface occurring in addition to the one observed in all previously reported double-D fragments. Thus, every γC domain is in contact with two other γC domains. Surprisingly, the cross-

[†] This work was supported by Grant HL-26873 from the National Heart, Lung and Blood Institute.

[‡] Atomic coordinates are available from the Protein Data Bank under the following access codes: 1N73 for lamprey DDGH, 1N86 for human DDX1, and 1N8E for human DDX2.

* To whom correspondence should be addressed. Telephone: (858) 534-4417. Fax: (858) 534-4985. E-mail: rdoolittle@ucsd.edu.

[§] Present address: Department of Biochemistry, Emory University School of Medicine, Atlanta, GA 30322.

10.1021/bi026666i CCC: $22.00
Published on Web 12/07/2002

links appear to involve γ chains separated by the novel D−D interface.

This observation might have been ascribed to an idiosyncrasy of the fibrinogen being from a very distantly related and primitive organism were it not for the fact that we found the same kind of double interfacing in crystal structures of two different double-D preparations prepared from human fibrin. One of these was a low-resolution structure of a putative "D2E" complex (but in the end not authentic D2E); the other was derived from a double-D preparation that had been cocrystallized with two long polypeptides patterned on the α- and β-chain amino-terminal segments of fibrin. Unfortunately, in both cases, the non-double-D material was degraded by contaminating proteases during the crystallization process. Nonetheless, in both cases, the presence of the surviving mixture of peptides led to a packing arrangement like that observed in the lamprey double-D in crystals.

The packing arrangement observed in a crystal need have no relationship to the native fibrin arrangement, of course. What was momentarily disconcerting was that the $\gamma-\gamma$ cross-linking in the lamprey system is at the newly observed interface (interface II) and not at the one commonly observed (interface I). Moreover, interface II has several intriguing features, including a natural symmetry and a favorable arrangement for the two γ-chain holes. What is clear in the end, however, is that the cross-links between D units are sufficiently flexible that, at least in the absence of fragment E, -either of the two interfaces can be accommodated, the choice during crystallization depending mainly on solution variables such as the presence of certain peptides. In this regard, we were able to gauge the extent of the cross-link flexibility by its limited vulnerability to proteases, a measure that correlated well with regions where the electron density begins to break up.

MATERIALS AND METHODS

Synthetic Peptides. Peptides were synthesized by the BOC method of Merrifield (*13*) on a Beckman 990 automatic synthesizer and cleaved from the resin by HF. These included a 27-residue peptide patterned on the amino terminus of the β-chain of human fibrin (GHRPLDKKREEAPALRPAPP-PIAGGGE). The peptide had initially been intended for use in affinity chromatography and included a glutamic acid at its carboxyl terminus to facilitate attachment to an amino resin. Also, two serines in the native sequence were replaced with alanines. Another synthetic peptide corresponded to the 12 amino-terminal residues of the α-chain of human fibrin (GPRVVERHQSAC). It was converted to the disulfide-linked bis-peptide, as occurs in the native molecule, by oxidation with ferricyanide followed by removal of inorganic byproducts on an anion exchange resin. Peptides were purified by reverse-phase HPLC on Vydac C-18 columns.

Residue Numbering. Residue numbering for vertebrate fibrinogens is most affected by the great variability in the lengths of fibrinopeptides A and B from different species. Lamprey fibrinogen represents an extreme case, having the shortest known A fibrinopeptide (only six residues) and one of the longest B fibrinopeptides (36 residues). On the other hand, γ-chains from all vertebrate fibrinogens are very similar, only an occasional small deletion or insertion affecting the numbering. These are the most important chains

```
                  380       385       390       395       400       405
lamprey γ chain   ..TTMKLLPMGRDLSGHGGQQQSKGNSRGDN
                    ||||  |   |  |     |||   |
human γ chain     ..TTMKIIPFNR-LTIGEGQQHHLGGAKQAGDV
                        385       390       395       400       405       410
```

FIGURE 1: Sequence comparison of the lamprey and human carboxyl-terminal regions of γ-chains involved in cross-linking by factor XIII. The putative glutamine and lysine residues involved in cross-linking are shown in bold. Note the differences in residue numbering between the lamprey and human chains.

in this study, however, and the sequence constituting the putative cross-linking segment in lamprey fibrinogen is compared with that from human fibrinogen in Figure 1. Because certain residues in the human structure are well-known for their functional importance, we often provide both kinds of numbering.

Lamprey Double-D. Lamprey fibrinogen was prepared from frozen lamprey plasma by a modified cold ethanol procedure (*14*). It was clotted with human thrombin (Enzyme Research) under conditions (10 mM cysteine, 10 mM calcium chloride, and 0.15 M NaCl) which favored cross-linking by residual factor XIII. Clots were left to stand for 3 h at 4 °C, after which the clot liquor was pressed out and the fibrin washed with 0.15 M NaCl, snipped with scissors, and suspended in a solution of human plasmin (0.06 mg/mL, Chromagenix). Digestion was allowed to continue for 6−8 h at 13 ° C, after which an appropriate amount of aprotinin (Trasylol) was added to stop the reaction. The double-D was obtained by affinity chromatography of the digest on a Gly-Pro-Arg-Pro affinity column (*15*, *16*) equilibrated with 0.15 M NaCl, 0.002 M $CaCl_2$, and 0.05 M imidazole (pH 7.0) and eluted with 1 M NaBr and 0.05 M sodium acetate (pH 5.3) containing 1.0 M urea. The urea was needed for elution because lamprey fragments D and double-D have a much stronger affinity for Gly-Pro-Arg than do D fragments from other species (*7*). The pooled peak fractions were quick-dialyzed to remove the bulk of the urea, after which they were concentrated by the addition of $^1/_3$ volume of saturated ammonium sulfate. The precipitate was dissolved in a minimal volume of 0.05 M Tris (pH 7.0) and 5 mM $CaCl_2$ and dialyzed against the same buffer to remove ammonium sulfate. Protein solutions (8−10 mg/mL) were stored at −70 °C. SDS−polyacrylamide gels revealed a single band of a 180 kDa product. Gels run under reducing conditions indicated that all γ-chains were present as covalent dimers.

Human Double-D. Human fibrinogen was prepared from outdated blood bank plasma and clotted with bovine thrombin (Parke-Davis) under conditions in which small amounts of contaminating factor XIII were sufficient to ensure cross-linking [0.15 M NaCl, 10 mM $CaCl_2$, and 10 mM cysteine (pH 7.0)]. Clots formed within 7−8 min, after which trypsin (Sigma) was added to a concentration of 0.05 mg/mL. Lysis occurred in a matter of hours, after which an excess of soybean trypsin inhibitor (Sigma) was added. The preparation was gel filtered on a Sephadex G-150 column (84 cm × 2.5 cm) equilibrated with 1.0 M NaBr and 0.05 M sodium acetate (pH 5.3) and then purified further by affinity chromatography on a Gly-Pro-Arg affinity column (*15*, *16*). SDS−polyacrylamide gels were used to monitor purity. This preparation was denoted HDDX1.

Human D2E. The complex of fragments known as D2E was prepared by clotting human fibrinogen with bovine thrombin under the conditions described above, except that

human plasmin (Kabi, final concentration of 0.012 mg/mL) was added just prior to gel formation, which occurred at 7 min. After 4 h, more plasmin (new final concentration of 0.018 mg/mL) was added and digestion allowed to continue for an additional 15 h, after which the preparation was centrifuged to remove traces of the undigested clot; aprotinin (Trasylol) was added to inhibit the plasmin. The D2E was prepared by fractional precipitation with ammonium sulfate, the initial fraction that precipitated at 30% saturation being discarded. Material precipitated at 50% saturation was redissolved in a smaller volume and the procedure repeated. The final precipitate was dissolved in 50 mM Tris (pH 7.0) and 5 mM $CaCl_2$, dialyzed against the same buffer, and stored in aliquots at −70 °C prior to crystallization. The presence of the D2E complex was ascertained by nondenaturing polyacrylamide gel electrophoresis. This preparation was denoted HDDX2.

Crystallizations. All crystals were grown by vapor diffusion from sitting drops at room temperature; PEG-3350 was used as a precipitant in all experiments. In the case of lamprey DDGH, solutions containing 6−8 mg/mL lamprey double-D, 50 mM Tris (pH 7.0), 4 mM GHRPam,[1] and 5 mM $CaCl_2$ were combined with an equal volume of 5.5% PEG and 50 mM Tris buffer (pH 7.0).

Human DDX1 double-D preparations [9 mg/mL in 0.05 M Tris (pH 7.0) and 5 mM $CaCl_2$] containing the disulfide-linked dodecamer peptide based on the amino-terminal sequence from the human fibrin α-chain, and the 27-mer based on the amino-terminal sequence of the fibrin β-chain, were mixed with equal volumes of 12% PEG-3350 containing 10 mM $CaCl_2$ and 50 mM Tris (pH 8.0). Before the preparation was mixed with well solution, the concentration of the α-chain bis-dodecapeptide was 400 μM; the concentration of the β-chain 27-mer was 640 μM. Crystals appeared in ∼2 weeks without seeding.

The human DDX2 preparation initially contained the complex "D2E". Crystallization drops were set by mixing equal volumes of the protein solution [10 mg/mL in 50 mM Tris (pH 7.0) and 5 mM $CaCl_2$] with 13.25% PEG-3350 containing 10 mM $CaCl_2$ and 50 mM Tris (pH 8.0). Fine needles were observed after ∼2 weeks. These were touch-seeded to fresh solutions, after which somewhat bigger needles appeared in ∼1 month. The process was repeated, after which large spar-like needles (up to 1 mm in length) developed during the next month. The crystals used for data collection were flash-frozen in 20% glycerol.

Data Collection. The diffraction data for LDDGH and HDDX1 were collected at the University of California at San Diego X-ray facility; the HDDX2 data were collected at the Stanford Synchrotron Radiation Source. Data from single, frozen specimens (either 20% glycerol or 15% MPD was used as a cryoprotectant) were used for the three different structure determinations. In all cases, data were processed with DENZO and SCALEPACK (*17*), and molecular replacement was carried out with AMORE (*18*). Extensive use was made of various programs in the CCP4 package (*19*). In the case of lamprey DDGH, a recently determined structure of lamprey fragment D was used as a search model (*12*) (PDB entry 1LWU). In the cases of the human double-D preparations (HDDX1 and HDDX2), a single fragment D domain from the human double-D structure (*9*) (PDB entry 1FZC) was used.

Table 1: Data Collection and Refinement Statistics for Lamprey DDGH, Human DDX1, and Human DDX2

	LDDGH	HDDX1	HDDX2
space group	*P*1	*P*212121	*P*212121
unit cell dimensions			
a (Å)	49.7	52.3	50.0
b (Å)	99.3	130.1	125.5
c (Å)	120.7	298.3	312.2
α (deg)	99.6	90.0	90.0
β (deg)	101.5	90.0	90.0
γ (deg)	92.4	90.0	90.0
no. of molecules per asymmetric unit	1	1	1
no. of crystals	1	1	1
highest resolution (Å)	2.9	3.1	4.5
no. of observations	75259	156847	71273
no. of unique reflections	40004	30589	10214
completeness (%)	81.7	79.8	83.4
completeness in the highest shell (%)	66.7	50.0	53.3
$R_{sym}(I)$ (%)[a]	0.084	0.131	0.138
mosaicity	0.75	0.55	0.80
refinement resolution range (Å)	15−2.9	20−3.2	20−4.5
no. of residues in protein	1544	1478	1482
no. of residues in model	1456 (94%)	1352 (91%)	1352 (92%)
R[b]	0.258	0.226	0.415
R_{free}[c]	0.308	0.289	0.416
rmsd for ideal bond lengths (Å)	0.008	0.008	−
rmsd for bond angles (deg)	1.41	1.46	−

[a] $R_{sym} = (\sum|I - \langle I\rangle|)/(\sum|I|)$. [b] Crystallographic R value $[\sum(||F_o| - |F_c||)/(\sum|F_o|)]$ with 95% of the native data for refinement. [c] R_{free} is the R value based on 5% of the native data withheld from refinement.

Model building was conducted with O (*20*) and refinement conducted with CNS (*21*); R_{free} (*22*) was used as a guide throughout. SigmaA-weighted electron density maps were constructed (*23*), including $|2F_o - F_c|$ and $|F_o - F_c|$ maps. Numerous cycles of rebuilding and refinement were conducted. NCS restraints were kept in place for all four βC and γC domains throughout the procedure (Table 1).

Modeling by Simulated Annealing. The electron density in some regions near the γ-chain carboxyl termini was not strong enough to trace both of the abutting chains with certainty. Accordingly, the entire molecules of the two linked D fragments were fixed in position up to position Rγ389 (lamprey numbering), after which simulated annealing was conducted on the remainder of the γ-chains (residues 390−408) without regard to the electron density. Additionally, the topology was set so that reciprocal connections between the glutamines at γ397 and the lysines at γ401 (lamprey numbering) were enforced. Slow cooling (CNS) was begun at a starting temperature of 5000 K with a cooling rate of 25 K per cycle. The simulation was carried out both with conditions of the relevant crystallographic symmetry and without. A similar strategy was used in the case of HDDX1, the entire molecule being fixed in place except for residues γ392−411 (human numbering) of the two contributing D fragments.

Buried surface areas were determined with the CCP4 areaimol routine, with the solvent and/or probe radius set to 1.4 Å.

[1] Abbreviations: GHRPam, Gly-His-Arg-Pro-amide; MPD, methylpentanediol.

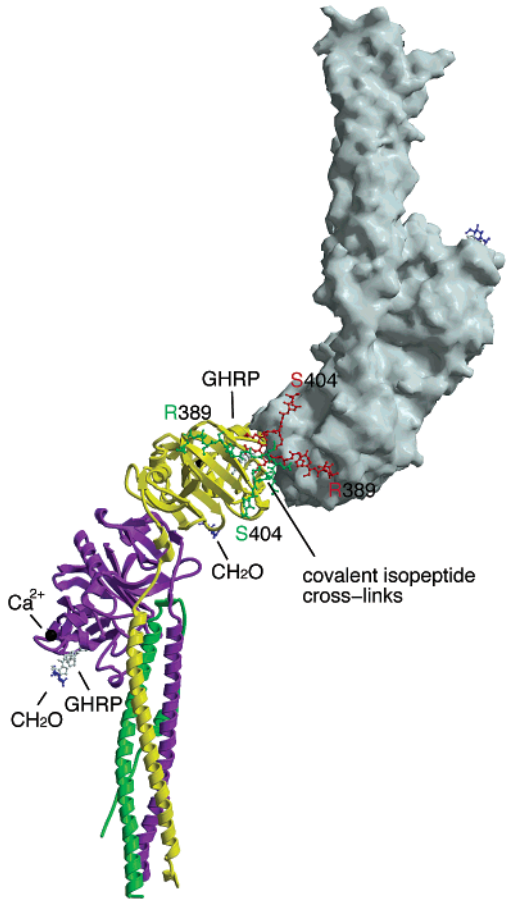

FIGURE 2: Model structure of lamprey fragment double-D complexed with the ligand GHRPam. One of the D units is shown in ribbon form (α-chain in green, *β*-chain in maroon, and *γ*-chain in yellow) except for the *γ*-chain cross-linking segment, which is shown as a green stick model. The other D unit is shown as a space-filled depiction except for the *γ*-chain cross-linking segment, which is shown as a red stick model. This figure was prepared with MolScript (*40*), GRASP (*41*), and Raster3D (*42*, *43*).

RESULTS

Overall Structure of LDDGH. A rotation search employing lamprey fragment DGH (PDB entry 1LWU) (*12*) as a search model yielded two solutions, consistent with there being a single dimeric molecule of double-D in the unit cell of the *P*1 space group. The calculated Matthews coefficient (*24*) was 3.3, indicating a relatively high solvent content of 63%. The structure, determined at 2.9 Å resolution (Table 1), was very similar to that reported for lamprey fragment D complexed with GHRPam. One exception was that in double-D the GHRPam ligand was found in both the *β*- and *γ*-chain holes (Figure 2). Consistent with this finding, the loop corresponding to residues *γ*357−361 in the double-D structure is folded in toward the binding site and not outward as was observed in the lamprey fragment D structure (*12*). Another significant difference between the structures occurs at the *γ*-chain carboxyl-terminal segment, the two being coincident only to *γ*-chain residue 391 (lamprey numbering). All other features, including calcium atoms and carbohydrate clusters, were virtually indistinguishable between the two structures.

Crystal Packing. The crystal packing in lamprey DDGH is different from what had been observed in previously reported double-D structures, two coincident, end-to-end, D−D interfaces being present (Figure 3). One of these, interface I, buries ∼450 Å^2 of surface area; the second, interface II, buries almost 1000 Å^2 of surface area, of which ∼400 Å^2 is contributed by the cross-linking segments. It involves a brace of loops consisting of residues *γ*294−299 and *γ*353−358 from one molecule interacting with residues *γ*372−376 and *γ*293−295, respectively, of the other. Several of these same loops are involved in side-by-side packing of *γ*-chain carboxyl domains in some other double-D crystal systems, although in a very different arrangement (*25*).

γ-Chain Cross-Linking. The existence of two different D−D interfaces in the same system presented a dilemma as to which two units were cross-linked. Surprisingly, the electron density indicated the joining of the two *γ*-chains across interface II (Figure 4). In this regard, the *γ*-chain could be traced on one side of the dimer as far as K*γ*401 (lamprey numbering; the human equivalent would be L*γ*403). Although the density on the opposite side of the interface faded after residue G*γ*395 (lamprey numbering; the human equivalent is G*γ*397), a model obtained by simulated annealing (see Materials and Methods) fell into good correspondence both with the density generated in an omit map and with its oppositely oriented mate (Figure 4). It should be noted that in lamprey fibrinogen the putative cross-link glutamine acceptor site is located at residue *γ*397 (lamprey numbering) and the putative lysine donor is at residue *γ*401.

The juxtaposition of the opposing carboxyl-terminal segments has an "over−under" form, one of the segments being in contact with the main body of the opposing *γ*-chain, but the other not (Figure 5). One of the contacts is a hydrogen bond between the side chain of Q*γ*398 from the C chain and D*γ*283 from the F chain; another may occur between *γ*Q399 (C chain) and D*γ*281 (F chain). These stabilizing contacts are likely what accounts for the electron density being so much better on the C chain side of the cross-link.

Structure of HDDX1. The human DDX1 preparation had been intended for crystallization of a double-D complex containing the bis-dodecameric peptide, simulating the connected pair of A knobs that exist at the α-chain amino termini of fibrin, and a 27-mer based on the sequence that exists at the amino terminus of fibrin *β*-chains. The structure, which was determined at 3.1 Å resolution, had a crystal packing system that was much the same as that observed in lamprey double-D with GHRPam.

The electron density at the *γ*-chain carboxyl termini extended, however weakly, to Q*γ*398 (human numbering), which, while not as extensive as in the case of lamprey double-D, still allowed the use of a simulated annealing strategy for gauging the general structure of the cross-links. As in the case of the lamprey form, the cross-links appear to bridge the *γ*-chains across the new kind of interface and do not occur across the conventional interface. As might be anticipated on the basis of the different positions of the cross-linking residues in the lamprey and human sequences, the chain paths are quite different in the two systems (Figure 6).

The crystal structure of HDDX1 revealed only a few remnants of the large peptides that had been included in the crystallization. In this regard, the *γ*-chain holes contained

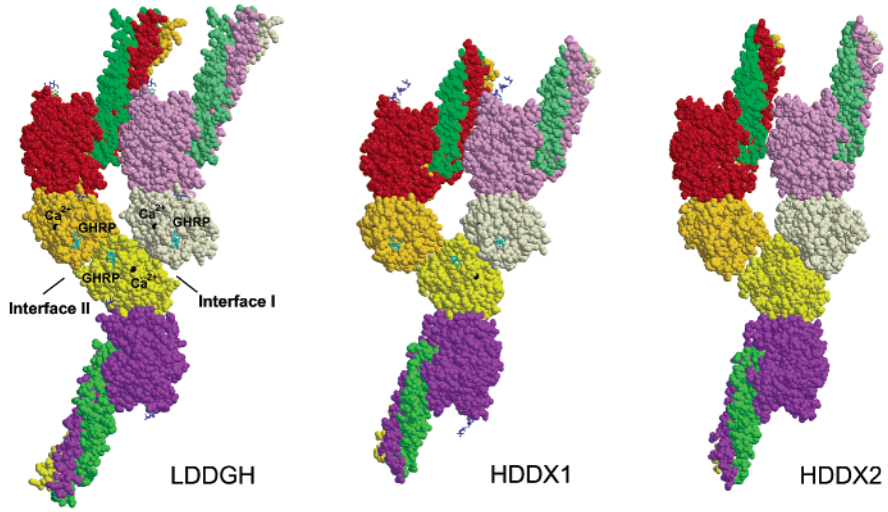

FIGURE 3: Comparison of the crystal packing of lamprey double-D complexed with GHRPam (LDDGH) with two human double-D preparations (DDX1 and DDX2) crystallized in the presence of complex assemblages of peptides. Two sets of $\gamma-\gamma$ interfaces exist in each case. Note that the projection for LDDGH has been rotated 180° relative to the view shown in Figure 2, thereby showing the GHRPam ligands and calcium atoms but not the cross-linking segments. This figure was prepared with MolScript (*40*) and Raster3D (*42*, *43*).

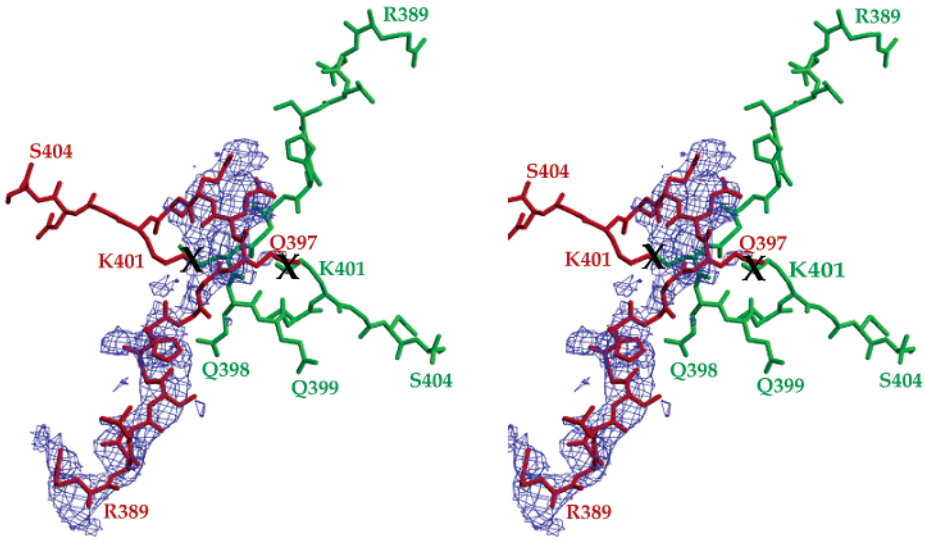

FIGURE 4: Stereo depiction of the electron density omit map ($|F_o - F_c|$ calculated at 1σ) for the cross-linking region in lamprey double-D. X's denote ϵ-amino-γ-glutamyl cross-links. Residues γ390−404 were not included in the model when calculating the map (see the text for details). This figure was prepared with XtalView (*44*) and Raster3D (*42*, *43*).

only Gly-Pro-Arg, the first three residues of the bis-dodecapeptide, the remainder being absent. Similarly, the first four residues of the 27-mer were clearly present in the β-chain holes; they were confirmed by the side chain positions of Eβ397 and Dβ398 being in the "flap in" position (*10*). There was no evidence of the remainder of the peptide. Subsequent experiments involving incubations set under the same conditions as the crystals revealed that both peptides were degraded within the course of 2 weeks.

Structure of HDDX2. The low-resolution data for HDDX2 were collected under the assumption that a long-sought complex of D2E had been crystallized. When the structure was determined at 4.5 Å resolution (Table 1), it was found that fragment E was not present. Subsequent experiments confirmed the presence of substantial contaminating protease activity. Apparently, the important amino-terminal sections of the fragment E were degraded during the extended crystallization period. What is of interest here, however, is that the crystal packing of this preparation was also like that observed in the lamprey DDGH system (Figure 3).

Accessibility of Cross-Linked Segments. Given that the same double-D preparation can be crystallized in forms in which the cross-linked domains employ different D−D interfaces, the following question arose: how constraining is the tether between the cross-linked segments? Put another way, how many residues reside in the flexible zone? In previous double-D structures (*1*, *9*, *10*), strong electron density in this region was observed to different extents, ranging from γ-chain residue γ393 to γ398 (human numbering), implying that this segment contained the general boundary for the region of flexibility. As a test of the accessibility of this region, we resorted to the longstanding method of probing with proteases (*26*). In this regard, we treated double-D preparations with trypsin in one set of experiments and with Staph V-8 protease (which cuts on the carboxyl sides of glutamic acid residues) in another. The potential targets included Rγ391 and Eγ396 in human preparations and the homologous Rγ389 in lamprey preparations; glutamic acid does not occur in this region of the lamprey γ-chain (Figure 1).

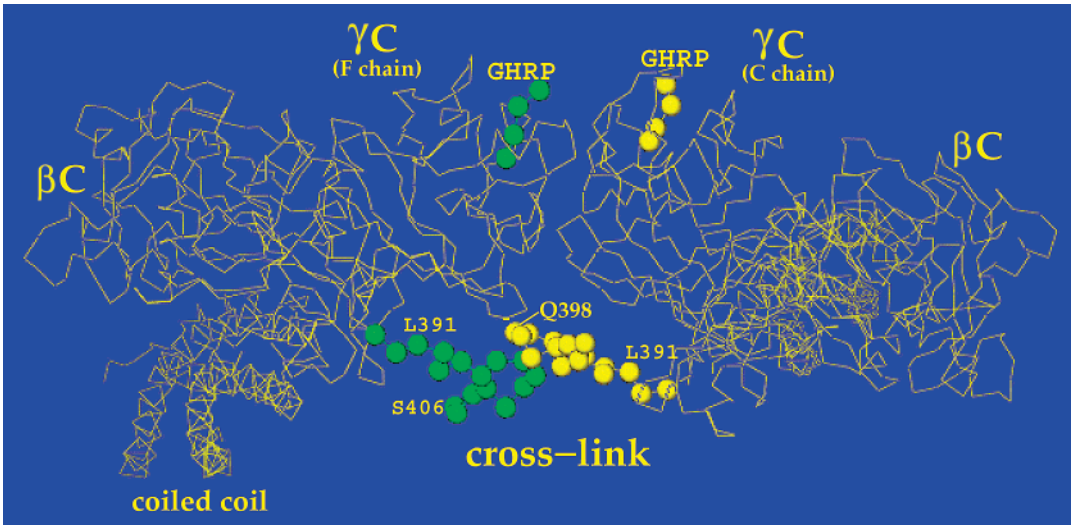

FIGURE 5: Over−under view of the cross-linking region in LDDGH. The cross-linked segments (residues γ389−404) are shown as spheres; those from the C chain are yellow, and those from the F chain are green. Note that Q398 of the C chain is in contact with the main body of the F chain. The GHRPam ligands are shown as spheres on the opposite side of the interface. The labeled coiled coil stretches toward the viewer; the second coiled coil is behind on the right side.

Under the conditions that were used [0.05 mg of trypsin/mL, 0.05 M imidazole (pH 7.0), and 0.005 M $CaCl_2$ at room temperature for 2 h], lamprey double-D was not cleaved at all by trypsin; human double-D was cleaved only to a small extent (Figure 7). Under equivalent conditions (0.05 mg of enzyme/mL, and same buffer, time, and temperature), Staph V-8 protease completely cleaved the human preparation to give a D-sized fragment (Figure 7). As expected, the lamprey preparation was not cleaved. These results are consistent with Rγ391 (human numbering) being in an unexposed location close to the folded domain and Eγ396 (human numbering) being in the exposed, flexible region. This means that the full extent of the cross-linked tether between units amounts to fewer than 20 residues in the case of lamprey and fewer than 24 in the case of human preparations. In either case, the tether would be loose enough to allow a choice of adjacent faces of the γC domain for packing during the crystallization process.

DISCUSSION

The D−D interface designated here as interface I invariably contributes to the crystal packing of human fragments D and double-D (*1*, *9*, *10*), as well as to crystals of lamprey fragment D (*12*), a modified bovine fibrinogen (*27*), and native chicken fibrinogen (*28*). It has been presumed that the cross-links in the double-D structures involved this interface, even though there was no corresponding electron density.

Interface I is asymmetric, the two participating molecules being arbitrarily assigned as A or B on the basis of the residues they contribute (*1*). In the human system, the A molecule is defined as the one that has Rγ275 interacting with Yγ280 of its B partner, the latter having its Rγ275 interacting with Sγ300 from its A partner. As it happens, although Rγ275 is conserved in the lamprey, both of the opposing residues are changed, without any apparent consequence (*12*).

The occurrence of a second interface, interface II, in crystals of a lamprey double-D preparation and two human double-D preparations was not surprising in itself; rather, it was the finding of the cross-link across the new interface that was at first unsettling. Upon reflection, however, we realized that previous crystal structures of human double-D do not have interface II and cannot possibly have their cross-links across it. The inescapable conclusion is that the linkage between the constituent D fragments is sufficiently flexible that different interfaces can exist under different environmental conditions.

The crystal structure of lamprey double-D presents the clearest picture so far of the cross-links themselves between joined D fragments. Although the electron density is only apparent on one side, it is in good correspondence with model segments generated by simulated annealing (Figure 4). Moreover, a similar result was obtained with a human double-D preparation (HDDX1), even though the corresponding human γ-chain segment is longer and has the cross-links further apart (Figures 1 and 6). In this regard, it should be remarked that others (*29*) have reported a somewhat different model for the cross-linking system by positioning 14-residue γ-chain model segments obtained from carrier-driven crystallization experiments across the D−D interface from an earlier human double-D structure. It should also be emphasized that the flexibility we have observed is much too limited to accommodate the so-called "transverse model" of γ-chain cross-linking that has been proposed by others (*30*).

Double-D and D2E. Some comments may be in order about the conditions used in the preparation of double-D, lest there be some misunderstanding about the starting material used to set crystal drops. In all cases, fibrinogen is clotted by thrombin in the presence of factor XIII such that clots are fully formed, virtually all γ chains being present as cross-linked dimers when examined on SDS gels. A variety of associative forces are at work in the mature clot, of course, including knob−hole interactions (D−E), end-to-end associations (D−D), and the interactions that bundle protofibrils together to form the mature fiber. These latter interactions likely utilize regions of the γC domain other than those at the D−D interface, as well as contributions from the βC (*25*) and αC domains (*31*). The destruction of

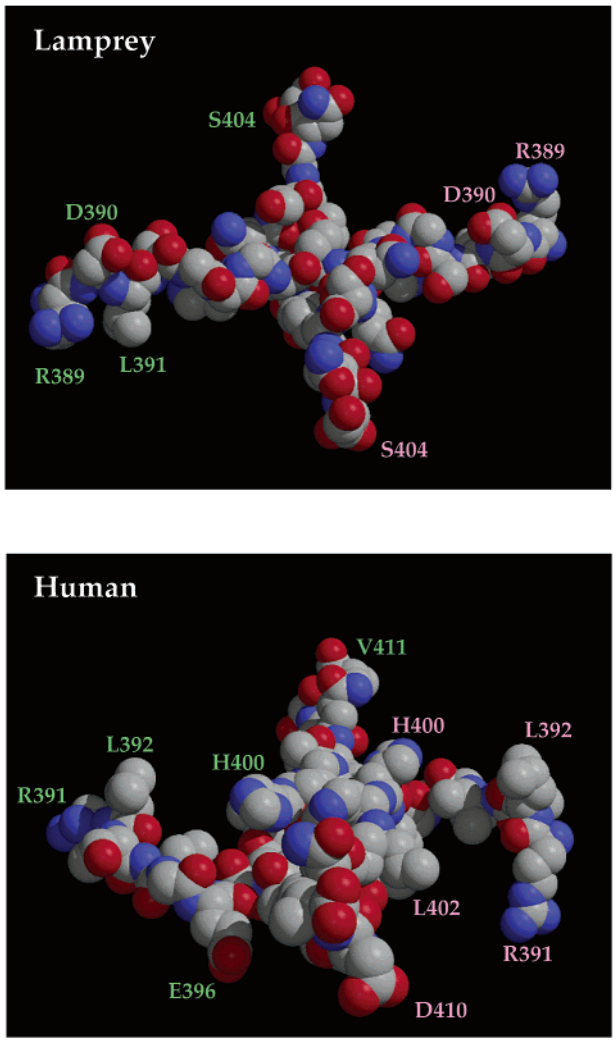

FIGURE 6: Space-filling models of cross-linking segments of LDDGH (residues γ391−404) (top) and HDDX1 (residues γ392−407) (bottom). Structures were calculated by simulated annealing without regard for electron density (see the text for details). In both cases, residues from the C chain are labeled in light green and those from the F chain in pink. See Figure 1 for sequence differences between lamprey and human γ-chains in this region. This figure was prepared with Raster3D (*42*, *43*).

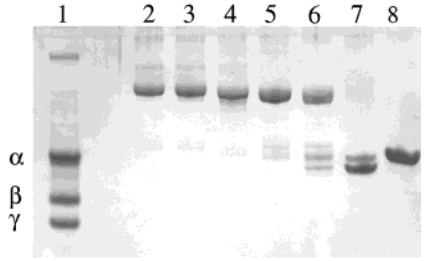

FIGURE 7: SDS−polyacrylamide gel showing cleavage of human double-D by Staph V-8 protease but not by trypsin. Lamprey double-D, which lacks a glutamate residue in this region, is not cleaved by Staph V-8 protease (see the text for details): lane 1, reduced human fibrinogen; lane 2, lamprey DD; lane 3, lamprey DD with trypsin; lane 4, lamprey DD with Staph V-8 protease; lane 5, human DD; lane 6, human DD with trypsin; lane 7, human DD with Staph V-8 protease; and lane 8, human fragment D.

the clot by plasmin, which occurs mainly by the cleavage and removal of αC domains and the severance of interdomainal coiled coils, leads to dissolution of the polymer and dissociation of the secondarily involved interfaces, the final core product being the complex D2E (*32*).

In the past, we have made countless attempts to crystallize the complex D2E. Indeed, it was our repeated failures in this endeavor that led us to the alternative route of removing the fragment E and supplying synthetic knobs instead (*1*). The separation of fragment E from double-D is readily accomplished by gel filtration in the presence of 1 M NaBr at pH 5.3, a classic environment well-known for its reversible depolymerization of fibrin (*33*).

Influence of Peptides. From the outset, it was apparent that the crystal packing of fragment D, and later double-D, was greatly affected by the presence of small peptides based on the amino-terminal segments of the α- and β-chains of fibrin, different unit cells, and space groups being observed (*34*). In all previous cases, however, only one end-to-end D−D interface was present.

Now we have found that lamprey double-D, in the presence of GHRPam, and human double-D, in the presence of a degenerate mix of peptides (for whatever reason), crystallize in such a way that two different but virtually equivalent D−D interfaces are present. The equivalence is well-illustrated by the arrangement of γ-chain holes, both pairs of which are perfectly situated for binding a pair of linked knobs on the face of the system that is diametrically opposite the cross-links (Figure 3).

Nevertheless, it seems most likely that interface I is the predominant D−D interface in native fibrin. This arrangement is strongly favored on several grounds, including the appearance of protofibrils in electron micrographs (*35*), the half-molecule periodicity of fibrin observed by electron microscopy (ref *36*, inter alia), and the particular nature of various polymerization defects in certain human variant fibrinogens (*37*−*39*). The D−D interfacial connection in fibrin may very well be loose, however, certainly allowing the ready interchange of the A−B to B−A interface across the asymmetric interface, and perhaps even the occasional switch to interface II.

In conclusion, cross-linked double-D preparations in solution are flexibly joined. How they crystallize depends on solution conditions that are especially sensitive to the kinds of peptide knobs present. It is possible that the presence of joined pairs of knobs bound into holes on adjacent units would limit the flexibility of the two covalently joined D fragments in a way that unlinked synthetic peptide knobs do not, but so far, we have been unable to obtain such crystals, with either fragment E or disulfide-linked dodecamers corresponding to A knob pairs.

ACKNOWLEDGMENT

We are grateful to Dr. Andrew Laudano for providing lamprey blood plasma and Dennis Olshefski and Yin Lin for assistance with peptide synthesis. We also thank Nick Nguyen at the University of California at San Diego X-ray facility for his able assistance and also the staff at the Stanford Synchrotron Radiation Laboratory for their cooperation during our visit.

REFERENCES

1. Spraggon, G., Everse, S. J., and Doolittle, R. F. (1997) *Nature 389*, 455−462.

2. Mosesson, M. W., and Doolittle, R. F., Eds. (1983) Molecular Biology of Fibrin and Fibrin, *Annals of the New York Academy of Sciences*, Vol. 408, New York Academy of Sciences, New York.
3. Nieuwenhuizen, W., Mosesson, M. W., and De Matt, P. M., Eds. (2001) *Annals of the New York Academy of Sciences*, Vol. 936, New York Academy of Sciences, New York.
4. Ferry, J. D. (1952) *Proc. Natl. Acad. Sci. U.S.A. 38*, 566−569.
5. Doolittle, R. F. (1984) *Annu. Rev. Biochem. 53*, 195−229.
6. Laudano, A. P., and Doolittle, R. F. (1978) *Proc. Natl. Acad. Sci. U.S.A.*
7. Laudano, A. P., and Doolittle, R. F. (1980) *Biochemistry 19*, 1013−1019.
8. Chen, R., and Doolittle, R. F. (1971) *Biochemistry 10*, 4486−4491.
9. Everse, S. J., Spraggon, G., Veerapandian, L., Riley, M., and Doolittle, R. F. (1998) *Biochemistry 37*, 8637−8642.
10. Everse, S. J., Spraggon, G., Veerapandian, L., and Doolittle, R. F. (1999) *Biochemistry 38*, 2941−2946.
11. Yee, V. C., Pratt, K. P., Cote, H. C., LeTrong, I., Chung, D. W., Davie, E. W., Stenkamp, R. E., and Teller, D. C. (1997) *Structure 5*, 125−138.
12. Yang, Z., Spraggon, G., Pandi, L., Everse, S. J., Riley, M., and Doolittle, R. F. (2002) *Biochemistry 41*, 10218−10224.
13. Merrifield, R. B. (1964) *Biochemistry 3*, 1385−1390.
14. Doolittle, R. F., Schubert, D., and Schwartz, S. A. (1968) *Arch. Biochem. Biophys. 118*, 456−467.
15. Kuyas, C., Haeberli, A., Walder, P., and Straub, P. W. (1990) *Thromb. Haemostasis 63*, 439−444.
16. Yamazumi, K., and Doolittle, R. F. (1992) *Proc. Natl. Acad. Sci. U.S.A. 89*, 2893−2896.
17. Otwinowski, Z., and Minor, W. (1997) *Methods Enzymol. 276*, 307−326.
18. Navaza, J. (1994) *Acta Crystallogr. A50*, 157−163.
19. Collaborative Computational Project Number 4 (1994) *Acta Crystallogr. D50*, 760−763.
20. Jones, T. A., Zou, J.-Y., Cowan, S. W., and Kjeldgaard, M. (1991) *Acta Crystallogr. A47*, 110−119.
21. Brunger, A. T., Adams, P. D., Clore, G. M., DeLano, W. L., Gros, P., Grosse-Kunstleve, R. W., Jiang, J.-S., Kuszewski, J., Nilges, M., Pannu, N. S., Read, R. J., Rice, L. M., Simonson, T., and Warren, G. L. (1998) *Acta Crystallogr. D54*, 905−921.
22. Brunger, A. T. (1992) *Nature 355*, 472−475.
23. Read, R. J. (1986) *Acta Crystallogr. A42*, 140−149.
24. Matthews, B. W. (1968) *J. Mol. Biol. 33*, 491−497.
25. Yang, Z., Mochalkin, I., and Doolittle, R. F. (2000) *Proc. Natl. Acad. Sci. U.S.A. 97*, 14156−14161.
26. Harrington, W. F., von Hippel, P H., and Mihalyi, E. (1959) *Biochim. Biophys. Acta 32*, 303−304.
27. Brown, J. H., Volkmann, N., Jun, G., Henschen, A. H., and Cohen, C. (2000) *Proc. Natl. Acad. Sci. U.S.A. 97*, 85−90.
28. Yang, Z., Kollman, J. M., Pandi, L., and Doolittle, R. F. (2001) *Biochemistry 40*, 12515−12523.
29. Ware, S., Donahue, J. P., Hawiger, J., and Anderson, W. F. (1999) *Protein Sci. 8*, 2663−2671.
30. Mosesson, M. W., Siebenlist, K. R., Hernandez, I., Wall, J. S., and Hainfield, J. F. (2002) *Thromb. Haemostasis 87*, 651−658.
31. Gorkun, O. V., Veklich, Y. I., Medved, L. V., Henschen, A. H., and Weisel, J. W. (1994) *Biochemistry 33*, 6986−6997.
32. Hudry-Clergeon, G., Patural, L., and Suscillon, M. (1974) *Pathol. Biol. 22* (Suppl.), 47−52.
33. Donnelly, T. H., Laskowski, M., Jr., Notley, N., and Scheraga, H. (1955) *Arch. Biochem. Biophys. 56*, 369−387.
34. Everse, S. J., Pelletier, H., and Doolittle, R. F. (1995) *Protein Sci. 4*, 1013−1016.
35. Williams, R. C. (1981) *J. Mol. Biol. 150*, 399−408.
36. Karges, H. E., and Kuhn, K. (1970) *Eur. J. Biochem. 14*, 94−97.
37. Everse, S. J., Spraggon, G., and Doolittle, R. F. (1998) *Thromb. Haemostasis 80*, 1−9.
38. Fellowes, A. P., Brennan, S. O., Ridgway, H., Heaton, D. C., and George, P. M. (1998) *Br. J. Haematol. 101*, 24−31.
39. Mullin, J. L., Brennan, S. O., Ganly, P. S., and George, P. M. (2002) *Haemostasis Thromb. Vasc. Biol. 99*, 3597−3601.
40. Kraulis, P. J. (1991) *J. Appl. Crystallogr. 24*, 946−950.
41. Nicholls, E. A., Sharp, K., and Honig, B. (1991) *Proteins*: *Struct., Funct., Genet. 11*, 281−296.
42. Bacon, D. J., and Anderson, W. F. (1988) *J. Mol. Graphics 6*, 219−220.
43. Merritt, E. A., and Murphy, M. E. P. (1994) *Acta Crystallogr. D50*, 869−873.
44. McRee, D. E. (1992) *J. Mol. Graphics 10*, 44−46.

BI026666I